

Supporting Material

Electronic, phononic, and superconducting properties of FeH_x ($x=1-6$) at 150 GPa

Hao Quan^{1,2,3*}, Shi-Na Li^{1*†}, Yu-Lin Han^{4‡}, Jian-Guo Si⁵, Wen-Xue Zhang⁶, Wei-Dong Li⁷, Bao-Tian Wang^{2,3§},

¹Institute of Theoretical Physics, State Key Laboratory of Quantum Optics and Quantum Optics Devices, Collaborative Innovation Center of Extreme Optics, Shanxi University, Taiyuan, 030006, PR China

²Institute of High Energy Physics, Chinese Academy of Science, Beijing 100049, PR China

³Spallation Neutron Source Science Center, Dongguan 523803, PR China

⁴School of Physics and Physical Engineering, Qufu Normal University, Qufu, 273165, PR China

⁵Songshan Lake Materials Laboratory, Dongguan, Guangdong 523808, PR China

⁶Institute of Laser Spectroscopy, State Key Laboratory of Quantum Optics and Quantum Optics Devices, Collaborative Innovation Center of Extreme Optics, Shanxi University, Taiyuan 030006, PR China

⁷Shenzhen Key Laboratory of Ultra Intense Laser and Advanced Material Technology, Center for Intense Laser Application Technology, and College of Engineering Physics, Shenzhen Technology University, Shenzhen 518118, PR China;

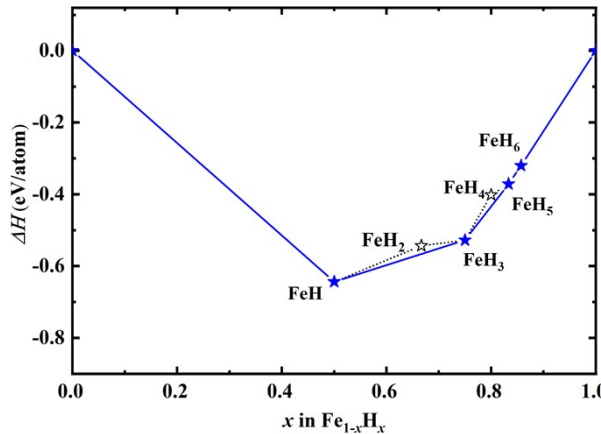


Fig. S1 Convex hull diagram with ZPE of FeH_x ($x=1-6$) at 150 GPa

Comparing Fig. S1 with Fig. 1 in the main manuscript, we find that the differences raised by including ZPE is limited. The only observable difference is the enthalpy difference (ΔH) of FeH_2 , which makes FeH_2 locate above the convex hull by 24 meV.

* These authors contributed equally to this work

† Corresponding author sqli@sxu.edu.cn

‡ Corresponding author 1624609643@qq.com

§ Corresponding author wangbt@ihep.ac.cn

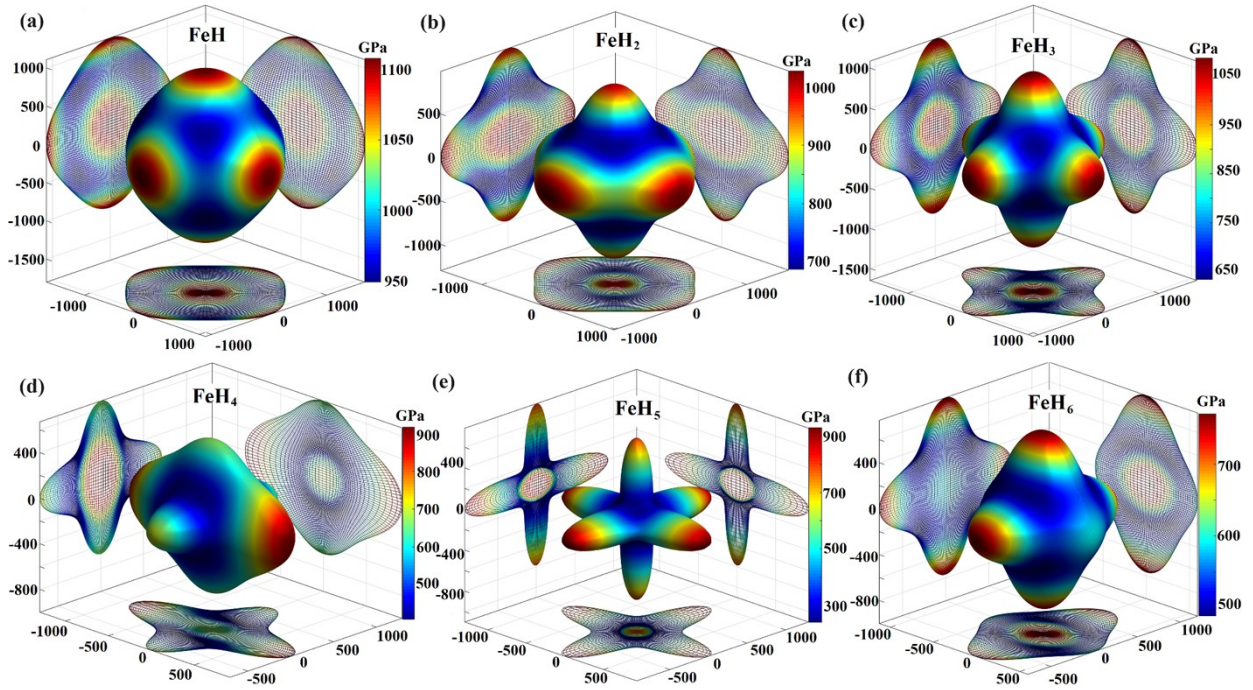


Fig. S2 3D directional dependent of Young's modulus for FeH_x ($x=1-6$) at 150 GPa.

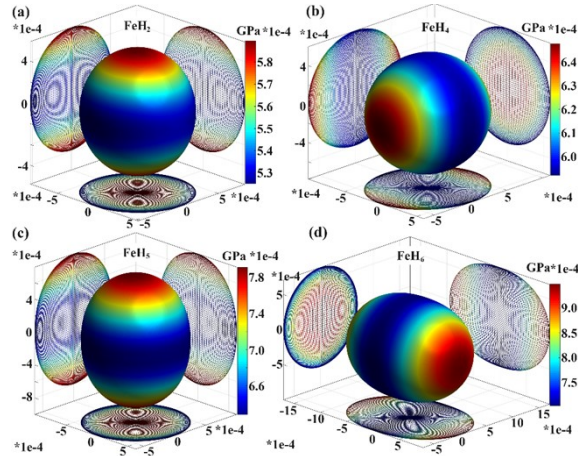


Fig. S3 3D directional dependent of linear compressibility β for (a) FeH_2 , (b) FeH_4 , (c) FeH_5 , and (d) FeH_6 at 150 GPa.

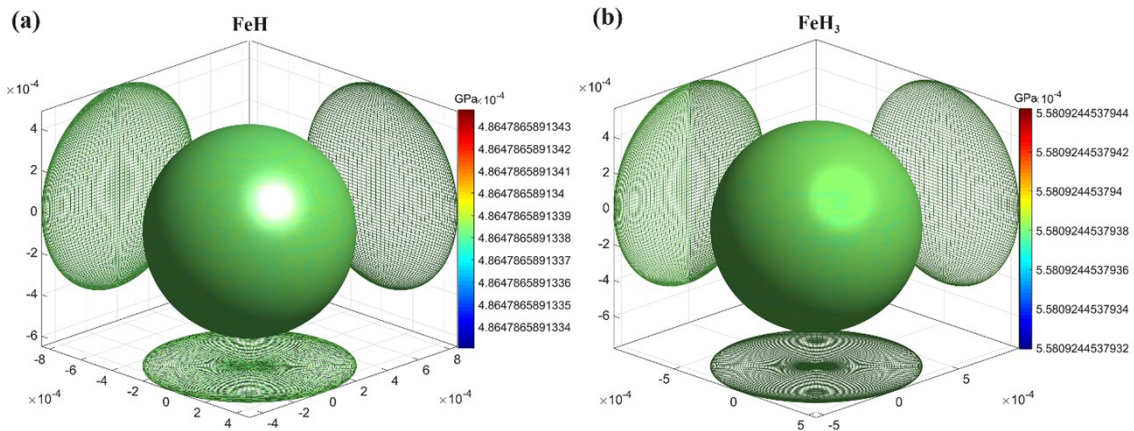


Fig. S4 Linear compressibility β of 3D graph for (a) FeH and (b) FeH_3 at 150 GPa.

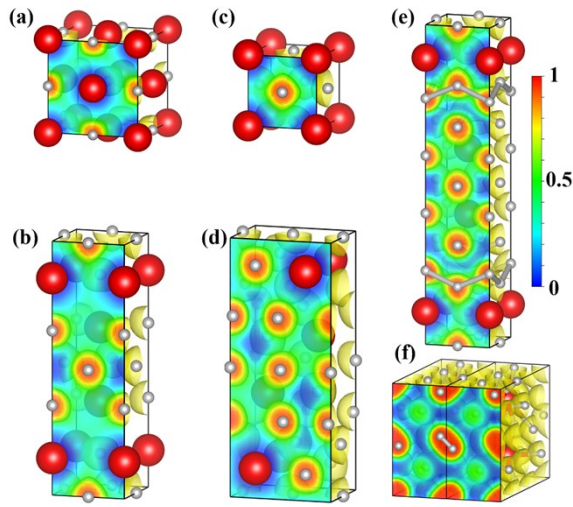


Fig. S5 Electron localization functions (ELF) of (a) FeH, (b) FeH₂, (c) FeH₃, (d) FeH₄, (e) FeH₅, and (f) FeH₆ (1×2×1 cell) at 150 GPa. Isosurface values are all set to 0.5.

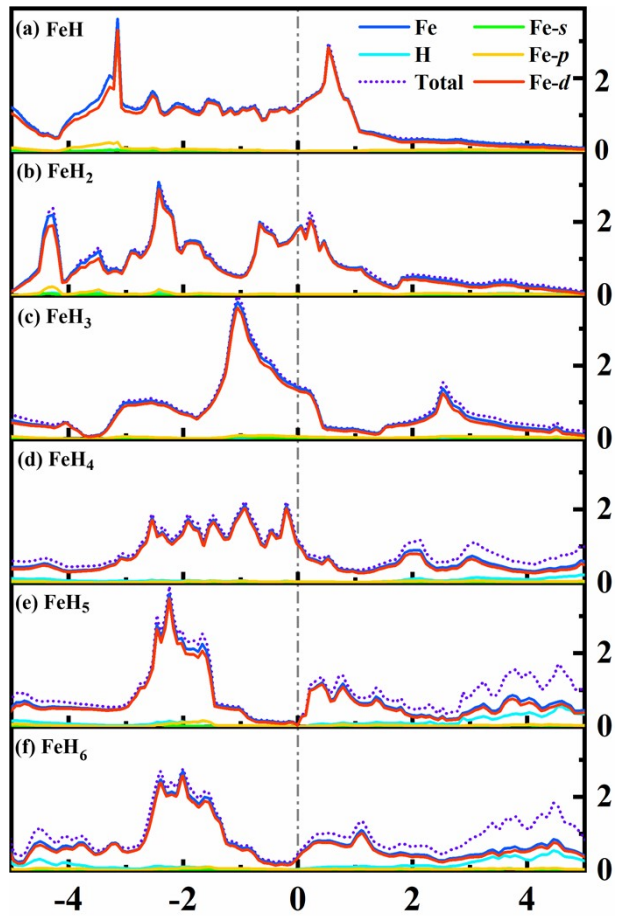


Fig. S6 (a) Density of states (DOS) of FeH_x ($x=1-6$) at 150 GPa.

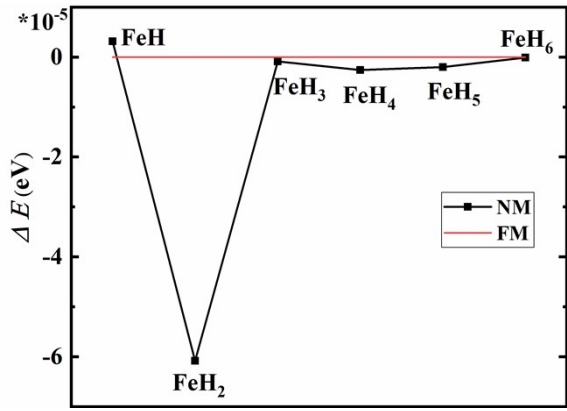


Fig. S7 Energy differences between different magnetic states of FeH_x ($x=1\text{-}6$) at 150 GPa.

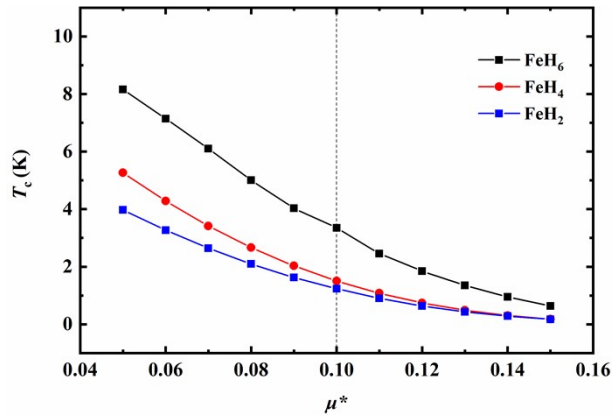


Fig. S8 Evaluated T_c of FeH_2 , FeH_4 , and FeH_6 as a function of Coulomb pseudopotential μ^* . Vertical line marks the value $\mu^* = 0.10$ used in this work.

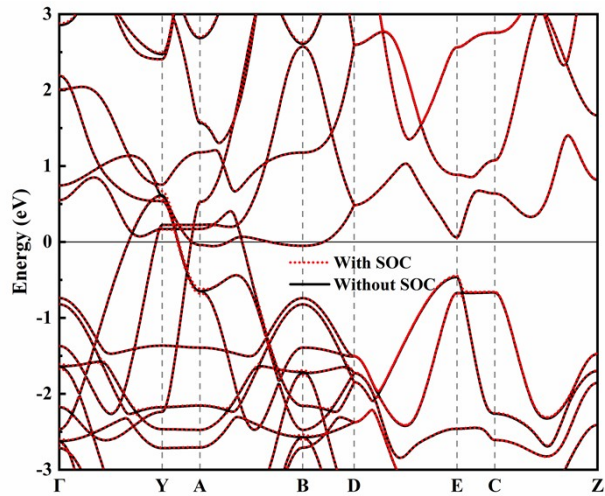


Fig. S9 Band structure of FeH_6 with and without SOC.

Table S1 Crystal structure details of FeH_x (x=1-6) at 150 GPa.

	Lattice parameters (Å, °)	Atom position		Distances Fe-H (Å)
FeH	$a=b=c=3.31$	Fe(4a)	(0.0,0.0,0.0)	
$Fm\bar{3}m$, Z=4	$\alpha=\beta=\gamma=90$	H(4b)	(0.5,0.5,0.5)	2.343
FeH ₂	$a=b=2.34$, $c=7.95$	Fe(4e)	(0.0,0.0,-0.146)	
$I4/mmm$, Z=4	$\alpha=\beta=\gamma=90$	H(4e)	(0.0,0.0,0.353)	1.658
		H(4e)	(0.0,0.5,0.0)	1.648
FeH ₃	$a=b=c=2.33$	Fe(1a)	(0.0,0.0,0.0)	
$Pm\bar{3}m$, Z=1	$\alpha=\beta=\gamma=90$	H(3c)	(0.5,0.5,0.0)	1.649
FeH ₄	$a=2.35$, $b=3.15$, $c=7.81$	Fe(4e)	(0.0,0.25,0.115)	
$Imma$, Z=4	$\alpha=\beta=\gamma=90$	H(4b)	(0.5,0.0,0.0)	1.676
		H(8h)	(0.0,0.974,0.300)	1.604
		H(4e)	(0.0,0.75,0.101)	1.579
FeH ₅	$a=b=2.39$, $c=11.51$	Fe(4e)	(0.0,0.0,0.897)	
$I4/mmm$, Z=4	$\alpha=\beta=\gamma=90$	H(8g)	(0.0,0.5,0.185)	1.523
		H(4e)	(0.0,0.0,0.410)	1.695
		H(4c)	(0.0,0.5,0.0)	1.680
		H(4e)	(0.0,0.0,0.230)	1.468
FeH ₆	$a=6.47$, $b=2.38$, $c=4.77$	Fe(4g)	(0.317,0.498,0.25)	
$P2/c$, Z=4	$\alpha=\beta=\gamma=90$	H(4g)	(0.665,0.0,0.499)	1.686
		H(4g)	(-0.0004,0.887,0.948)	2.436
		H(4g)	(0.911,0.537,0.250)	1.476
		H(4g)	(0.169,-0.0003,0.251)	1.530
		H(4g)	(0.161,0.5003,0.0001)	1.526
		H(2b)	(0.5,0.5,0.0)	1.675
		H(2f)	(0.5,-0.0002,0.75)	1.681

Table S2 Minimum and maximum value of Young's modulus E and linear compressibility β for FeH_x ($x=1-6$) at 150 GPa.

	E_{min}	E_{max}	E_{min}/E_{max}	β_{min}	β_{max}	β_{min}/β_{max}
FeH	948.57	1108.31	0.86	0.48	0.48	1.00
FeH ₂	687.51	1027.01	0.67	0.52	0.58	0.90
FeH ₃	633.75	1087.04	0.58	0.55	0.55	1.0
FeH ₄	407.34	917.49	0.44	0.59	0.64	0.91
FeH ₅	239.98	929.96	0.26	0.63	0.76	0.84
FeH ₆	488.85	769.80	0.64	0.70	0.95	0.73

Cubic

C_{11} , C_{12} and C_{44} .

Bron-Huang mechanical stability criterion:

$$C_{11} - C_{12} > 0, C_{44} > 0, C_{11} + 2C_{12} > 0 \quad (1)$$

Tetragonal

C_{11} , C_{12} , C_{13} , C_{33} , C_{44} and C_{66} .

Bron-Huang mechanical stability criterion:

$$C_{11} - C_{12} > 0, C_{11} + C_{33} - 2C_{13} > 0, C_{11} > 0, C_{33} > 0, C_{44} > 0, C_{66} > 0 \quad (2)$$

Orthorhombic

C_{ii} ($i=1-6$), C_{12} , C_{13} , C_{23} ;

Bron-Huang mechanical stability criterion:

$$C_{ii} > 0 \quad (i=1,2,3,4,5,6), \quad (C_{11} + C_{22} - 2C_{12}) > 0, \quad (C_{11} + C_{33} - 2C_{13}) > 0$$

$$(C_{22} + C_{33} - 2C_{23}) > 0, \quad [C_{11} + C_{22} + C_{33} + 2(C_{12} + C_{13} + C_{23})] > 0 \quad (3)$$

Monoclinic

C_{ii} ($i=1-6$), C_{i5} ($i=1-3$), C_{12} , C_{13} , C_{23} and C_{46} .

Bron-Huang mechanical stability criterion:

$$\begin{aligned} C_{11} &> 0, C_{44} > 0, C_{11}C_{22} > C_{12}^2, C_{44}C_{66} > C_{46}^2 \\ C_{15}^2(C_{23}^2 - C_{22}C_{33}) &+ C_{25}^2(C_{13}^2 - C_{11}C_{33}) + C_{35}^2(C_{12}^2 - C_{11}C_{22}) \\ + 2C_{15}C_{35}(C_{13}C_{22} &- C_{12}C_{33}) + 2C_{15}C_{25}(C_{12}C_{33} - C_{13}C_{23}) + 2C_{25}C_{35}(C_{23}C_{11} - C_{12}C_{13}) \\ + \Delta C_{55} &> 0 \end{aligned} \quad (4)$$

$$\Delta = C_{11}C_{22}C_{33} + 2C_{12}C_{13}C_{23} - C_{11}C_{23}^2 - C_{22}C_{13}^2 - C_{33}C_{12}^2 > 0$$

E and β depending on the crystal orientation:

Cubic phase (for FeH and FeH₃):

$$\frac{1}{E} = s_{11} - 2(s_{11} - s_{12} - \frac{1}{2}s_{44})(l_1^2 l_2^2 + l_2^2 l_3^2 + l_3^2 l_1^2) \quad \beta = (s_{11} + 2s_{12}) \quad (5)$$

Tetragonal phase (for FeH₂ and FeH₅):

$$\begin{aligned} \frac{1}{E} &= (l_1^4 + l_2^4)s_{11} + l_3^4 s_{33} + l_1^2 l_2^2(2s_{12} + s_{66}) + l_3^2(1 - l_3^2)(2s_{13} + s_{44}) \\ \beta &= (s_{11} + s_{12} + s_{13}) - (s_{11} + s_{12} - s_{13} - s_{33})l_3^2 \end{aligned} \quad (6)$$

Orthorhombic phase (for FeH₄)

$$\frac{1}{E} = l_1^4 s_{11} + 2l_1^2 l_2^2 s_{12} + 2l_1^2 l_3^2 s_{13} + l_2^4 s_{22} + 2l_2^2 l_3^2 s_{23} + l_3^4 s_{33} + l_2^2 l_3^2 s_{44} + l_1^2 l_3^2 s_{55} + l_1^2 l_2^2 s_{66}$$

$$\beta = (s_{11} + s_{12} + s_{13})l_1^2 + (s_{12} + s_{22} + s_{23})l_2^2 + (s_{13} + s_{23} + s_{33})l_3^2 \quad (7)$$

Monoclinic phase (for FeH₆)

$$\begin{aligned} \frac{1}{E} = & l_1^4 s_{11} + 2l_1^2 l_2^2 s_{12} + 2l_1^2 l_3^2 s_{13} + 2l_1^2 l_2 l_3 s_{14} + 2l_1^3 l_3 s_{15} + 2l_1^3 l_2 s_{16} + \\ & l_2^4 s_{22} + 2l_2^2 l_2^2 s_{23} + 2l_2^3 l_3 s_{24} + 2l_1 l_2^2 l_3 s_{25} + 2l_1 l_2^3 s_{26} + l_3^4 s_{33} + 2l_2 l_3^2 s_{34} + 2l_1 l_3^3 s_{35} + 2l_1 l_2 l_3^2 s_{36} + \\ & l_2^2 l_3^2 s_{44} + 2l_1 l_2 l_3^2 s_{45} + 2l_1 l_2^2 l_3 s_{46} + l_1^2 l_3^2 s_{55} + 2l_1^2 l_2 l_3 s_{56} + l_1^2 l_2^2 s_{66} \end{aligned}$$

$$\beta = (s_{11} + s_{12} + s_{13})l_1^2 + (s_{12} + s_{22} + s_{23})l_2^2 + (s_{13} + s_{23} + s_{33})l_3^2 + (s_{15} + s_{25} + s_{35})l_3 l_1 \quad (8)$$

s_{ij} is the elastic compliance matrix and l_1 , l_2 , and l_3 are the direction cosines in any arbitrary direction.

High symmetry points coordinate:

Fm $\bar{3}$ m/Pm $\bar{3}$ m

0.0000000000	0.0000000000	0.0000000000	Γ
0.5000000000	0.0000000000	0.5000000000	X
0.5000000000	0.5000000000	0.0000000000	M
0.0000000000	0.0000000000	0.0000000000	Γ
0.5000000000	0.5000000000	0.5000000000	R
0.0000000000	0.5000000000	0.0000000000	Z

I4/mmm

0.0000000000	0.0000000000	0.0000000000	Γ
0.0000000000	0.5000000000	0.0000000000	X
0.5000000000	0.5000000000	0.0000000000	M
0.0000000000	0.0000000000	0.0000000000	Γ
0.0000000000	0.0000000000	0.5000000000	Z
0.0000000000	0.5000000000	0.5000000000	R
0.5000000000	0.5000000000	0.5000000000	A
0.0000000000	0.0000000000	0.5000000000	Z
0.0000000000	0.5000000000	0.0000000000	X
0.0000000000	0.5000000000	0.5000000000	R
0.5000000000	0.5000000000	0.0000000000	M
0.5000000000	0.5000000000	0.5000000000	A

Imma

0.0000000000	0.0000000000	0.0000000000	Γ
0.0000000000	0.0000000000	0.5000000000	Z
0.0000000000	0.5000000000	0.5000000000	T
0.0000000000	0.5000000000	0.0000000000	Y
0.5000000000	0.5000000000	0.0000000000	S
0.5000000000	0.0000000000	0.0000000000	X
0.5000000000	0.0000000000	0.5000000000	U
0.5000000000	0.5000000000	0.5000000000	R

P2/c

0.0000000000	0.0000000000	0.0000000000	Γ
0.0000000000	0.5000000000	0.0000000000	Y
-0.5000000000	0.5000000000	0.0000000000	A
-0.5000000000	0.0000000000	0.0000000000	B
-0.5000000000	0.0000000000	0.5000000000	D
-0.5000000000	0.5000000000	0.5000000000	E
0.0000000000	0.5000000000	0.5000000000	C
0.0000000000	0.0000000000	0.5000000000	Z